Mol Neurobiol (2017) 54:1–14
DOI 10.1007/s12035-015-9635-y

Enhanced Therapeutic Potential of Nano-Curcumin Against Subarachnoid Hemorrhage-Induced Blood–Brain Barrier Disruption Through Inhibition of Inflammatory Response and Oxidative Stress

Zong-yong Zhang[1] · Ming Jiang[2] · Jie Fang[1] · Ming-feng Yang[1] · Shuai Zhang[1] · Yan-xin Yin[2] · Da-wei Li[1] · Lei-lei Mao[1] · Xiao-yan Fu[1] · Ya-jun Hou[1] · Xiao-ting Fu[1] · Cun-dong Fan[1] · Bao-liang Sun[1]

Received: 14 July 2015 / Accepted: 15 December 2015 / Published online: 26 December 2015

Abstract Curcumin and nano-curcumin both exhibit neuroprotective effects in early brain injury (EBI) after experimental subarachnoid hemorrhage (SAH). However, the mechanism that whether curcumin and its nanoparticles affect the blood–brain barrier (BBB) following SAH remains unclear. This study investigated the effect of curcumin and the poly(lactide-co-glycolide) (PLGA)-encapsulated curcumin nanoparticles (Cur-NPs) on BBB disruption and evaluated the possible mechanism underlying BBB dysfunction in EBI using the endovascular perforation rat SAH model. The results indicated that Cur-NPs showed enhanced therapeutic effects than that of curcumin in improving neurological function, reducing brain water content, and Evans blue dye extravasation after SAH. Mechanically, Cur-NPs attenuated BBB dysfunction after SAH by preventing the disruption of tight junction protein (ZO-1, occludin, and claudin-5). Cur-NPs also upregulated glutamate transporter-1 and attenuated glutamate concentration of cerebrospinal fluid following SAH. Moreover, inhibition of inflammatory response and microglia activation both contributed to Cur-NPs' protective effects. Additionally, Cur-NPs markedly suppressed SAH-mediated oxidative stress and eventually reversed SAH-induced cell apoptosis in rats. Our findings revealed that the strategy of using Cur-NPs could be a promising way in improving neurological function in EBI after experimental rat SAH.

Keywords Subarachnoid hemorrhage · Nano-curcumin · Early brain injury · Blood–brain barrier · Oxidative stress · Apoptosis

Zong-yong Zhang, Ming Jiang and Jie Fang contributed equally to this work.

✉ Zong-yong Zhang
zongyongzhanghust@163.com

✉ Cun-dong Fan
tsmc_nks@tsmc.edu.cn

✉ Bao-liang Sun
blsun88@163.com

[1] Key Lab of Cerebral Microcirculation in Universities of Shandong, Taishan Medical University, Taian, Shandong 271000, China

[2] Biomedical Research Center of Tongji University Suzhou Institute, 215101 Suzhou, Jiangsu, China

Introduction

Aneurysmal subarachnoid hemorrhage (SAH) is a fatal form of stroke and leads to death or long-lasting neurological or cognitive impairment for survivors [1]. Recent authoritative opinions suggest that early brain injury (EBI), which refers to the acute injuries to the brain within the first 72 h after SAH, is considered as the primary cause of high disability and mortality rate in SAH patients [2, 3]. A range of physiological derangements that occur in EBI, such as glutamate neurotoxicity, inflammatory response, and oxidative stress, have been implicated in the disruption of the blood–brain barrier (BBB), development of brain edema, and secondary neuronal injury after SAH [4]. In experimental SAH, glutamate concentration of cerebrospinal fluid (CSF) was significantly high, while expression of glutamate transporter-1 (EAAT-2, also known as GLT-1) obviously reduced [5]. The neurotoxicity effect-mediated excessive glutamate contains excessive activation of ionotropic and metabotropic glutamate receptors leading to massive Ca^{2+} influx and subsequent apoptosis and necrosis,

promoting an excessive influx of sodium secondary to cell swelling and edema [6]. Oxidative stress-induced protein breakdown, lipid peroxidation, and DNA damage cause the damage elements of the neurovascular unit and mediate the neuroinflammation, BBB disruption, and production of spasmogen after SAH [7]. Neuroinflammation is a driving force behind the pathology of SAH, contributing to brain edema, BBB disruption, vasospasm, and neuronal loss. Excessive amounts of proinflammatory cytokines released by activated microglia, together with microglial signaling-induced astrocyte cytotoxicity, become deleterious to surrounding cells or neighboring neurons after SAH [8].

Curcumin, a hydrophobic polyphenol from the rhizomatous of the plant *Curcuma longa*, exhibits a wide variety of anti-inflammatory, anti-oxidant, anti-carcinogenic, and antiviral activities [9]. Although curcumin is a promising compound with neuroprotective effect, its utility is greatly limited by its poor brain bio-availability due to poor absorption, high rate of metabolism, and systemic elimination [10]. The poly(lactide-co-glycolide) (PLGA) is a bio-compatible and bio-degradable copolymer, which has been approved by the Food and Drug Administration (FDA) as a therapeutic device and has been reported as a carrier of raw curcumin through oral administration increasing bio-availability of curcumin [11, 12]. Previous studies showed that curcumin reduces vascular inflammation and cerebral vasospasm in the endovascular perforation mouse SAH model [13] and attenuates glutamate neurotoxicity and oxidative stress in the double-hemorrhage rat SAH model [14]. The nano-sized PLGA-encapsulated curcumin down-regulates NF-κB and decreases caspase-9a expression and CSF levels of TNF-α and IL-1β in the double-hemorrhage rat SAH model [15]. However, it is not known whether curcumin and nanocurcumin affects BBB disruption after SAH.

In the present study, we aim to investigate the influence of curcumin and PLGA-encapsulated curcumin nanoparticles (Cur-NPs) on BBB disruption and the possible mechanism (glutamate neurotoxicity, inflammatory response, oxidative stress, and cell apoptosis) underlying BBB dysfunction in EBI after SAH using the endovascular perforation rat SAH model.

Materials and Methods

Animals and Experimental Design

The 12-week-old male Sprague Dawley rats (260–300 g) were purchased from Vital River Laboratory Animal Center (Beijing, China). Rats were group-housed with a 12-h light/dark cycle. All procedures were in accordance with the National Institutes of Health guideline and were approved by the Taishan Medical University Animal Care and Use Committee.

The animals were divided randomly into six groups: sham-operated group ($n=24$), vehicle-treated SAH group ($n=24$), curcumin-treated SAH group (150 mg/kg, $n=24$; 300 mg/kg, $n=24$); and Cur-NP-treated SAH group (10 mg/kg, $n=30$; 10 mg/kg, $n=30$). Eighteen rats of each group were for measuring mortality rate analysis (at 24 and 48 h), neurological assessment (at 24 h), glutamate concentration in CSF (at 48 h), lactate dehydrogenase (LDH) activity, and release of cyochrome c (at 48 h). Six rats of each group were for detecting brain water content and BBB permeability at 24 h. Six rats of the Cur-NP-treated SAH group were for molecular biological and biochemical experiments at 24 h. Three rats of the Cur-NP-treated SAH group were for immunohistological staining at 24 h.

Rat SAH Model

Experimental SAH was induced by intracranial endovascular perforation as previously described [16]. After an incision of the ventral neck, the right external carotid artery (ECA) was transected distally and reflected caudally in line with the internal carotid artery (ICA). A blunted 4–0 nylon monofilament suture was introduced through the right ECA stump into the ICA until resistance was felt. The suture was pushed approximately 3 mm further penetrating the bifurcation of the anterior and middle cerebral artery (MCA). Then, the suture was withdrawn rapidly, to allow reperfusion of the ICA and inducing experimental SAH.

The SAH severity was quantified as previously described [16]. Briefly, the picture of the brain was taken and divided into six segments. Each segment was scored (0–3) depending on the amount of subarachnoid blood. Score of 0 means no subarachnoid blood; score of 1, minimal subarachnoid blood; score of 2, moderate blood with visible arteries; and score of 3, blood clot covering all arteries within the segment. A total score (0–18) was calculated as the sum of six segments.

Preparation of Curcumin-Loaded PLGA Nanoparticles

Cur-NPs were prepared as described previously [17–19], with slight modifications. Briefly, curcumin (5 mg) and PLGA (50 mg) were dissolved in dichloromethane (1.25 ml). The curcumin and PLGA solution (1 ml) was mixed with 10 % (*w*/*v*) polyvinyl alcohol (PVA) surfactant solution (2 ml) and sonicated (60 W, 5 min, on ice) to form an oil-in-water emulsion. The formed emulsion was dispersed in 0.5 % (*w*/*v*) PVA solution and stirred for 12 h at room temperature to allow evaporation of organic solvent. The prepared nanoparticles were collected by centrifugation (13,000 rpm, 30 min) and washed with distilled water to remove PVA and unencapsulated curcumin.

Particle Size, Entrapment Efficiency, Zeta Potential, In Vitro Drug Release Study of Cur-NPs

The morphology and particle size of Cur-NPs were observed by transmission electron microscopy (TEM, Hitachi) as described previously [17]. A dilute solution of Cur-NPs (1:10 dilution) was prepared. One drop (100 μl) of this solution was placed on the grid of TEM for 20 min, then washed twice with double-distilled water and allowed to dry. The photos were captured at an accelerating voltage of 120 kV under a microscope. To determine the entrapment of efficiency of Cur-NPs, the standard concentration of curcumin and the amount of non-encapsulated curcumin were measured at an absorption value of OD430 nm by a microplate reader. Entrapment of efficiency was calculated by (total amount of curcumin − non-encapsulated curcumin) / total × 100 % as described previously [17]. The zeta potential of Cur-NPs was determined using a Zeta potential analyzer. The in vitro drug release study of Cur-NPs was evaluated by the dialysis method as described previously [19]. Cur-NPs (10 mg) were dispersed in 50 % ethanol (1 ml), then solution was transferred to the 12-kDa molecular weight-cutoff dialysis bag, dialyzed against 50 % ethanol (60 ml) and stirred (50 rpm) at 37 °C. At a predetermined time, 1 ml of sample was withdrawn and measured at OD430 nm by a microplate reader and the sample amount of fresh medium was added to the dialysis bag.

Drug Administration

In the curcumin-operated group, at 30 min after operation, rats received daily single intraperitoneal (i.p.) injections of curcumin (150, 300 mg/kg body weight in corn oil) or vehicle (corn oil) of equal volume. Dosage and time of curcumin administration were based upon prior investigation in mice model of SAH [13]. In Cur-NP-operated group, at 30 min after operation, rats received daily single intraperitoneal (i.p.) injections of Cur-NPs (10, 20 mg/kg body weight in saline) or equal-volume vehicle (saline). Dosage and time of Cur-NP administration were based upon prior investigation in rat model of Alzheimer's disease [19].

Neurological Deficits

The neurological deficits were evaluated using a modified Garcia scoring system [16]. The assessment consisted of six tests that were scored 0–3 or 1–3 (spontaneous activity; symmetry in the movement of all four limbs; forepaw outstretching; climbing; body proprioception; and response to whisker stimulation). The total score ranged from 3 to 18. Neurological score was evaluated at 24 h after SAH.

Brain Water Content and BBB Permeability

Brain water content was measured as (wet weight − dry weight) / wet weight × 100 % according to our previous study [20]. Rats were sacrificed at 24 h after SAH. Brains were taken and separated into the left hemisphere, right hemisphere, cerebellum, and brain stem. The specimens were weighed immediately (wet weight) and dried at 100 °C for 48 h (dry weight).

BBB permeability was assessed by Evans blue extravasation at 24 h after SAH according to our previous study [21]. Two percent (*w*/*v*) of Evans blue (EB, Sigma) was given intravenously and allowed to circulate for 1 h. Rat was perfused transcardially with phosphate-buffered saline (PBS) to remove remaining intravascular EB dye. Brain was weighed and homogenized in PBS and then centrifuged. The supernatant was mixed with an equal volume of trichloroacetic acid with ethanol (1:3). After overnight incubation, the sample was centrifuged and the supernatant was measured at OD610 nm by a microplate reader.

Western Blot Analysis

The right hemispheres of brain were harvested at 24 h after SAH and performed according to our previous study [20, 21]. In brief, the right cortical sample was homogenized and centrifuged. An equal protein amount of each sample was added in a loading buffer, denatured and separated by 8–12 % (*v*/*v*) SDS gel, and transferred to nitrocellulose membranes. Membranes were blocked with 5 % nonfat dry milk and incubated with primary antibody (VEGF, sc-507; MMP9, sc-6841; ZO-1, sc-8147; occludin, sc-8144; claudin-5, sc-28670; β-actin, sc-47778; ED-1, sc-59103; Bcl-2, sc-783; Bax, sc-6236, Santa Cruz Biotechnology; EAAT2, ab41621; active caspase-3, ab2302, Abcam). Then, membranes were treated with anti-rabbit/mouse IgG horseradish peroxidase (HRP)-linked secondary antibody and were detected by chemiluminescence substrate (Thermo Scientific) and visualized by using ChemiDoc™ MP Imaging System (Bio-Rad). The density of protein bands was quantified using ImageJ software.

Measurement of Glutamate Concentration in CSF

Samples of CSF were collected at 24 or 48 h after surgery and frozen at −80 °C until assayed. Glutamate concentration in CSF was measured using glutamate assay kit for rats according to the manufacturer's instructions (BioVision). Briefly, test samples and glutamate standard were added with assay buffer in a 96-well plate (50 μl/well), mixed with the reaction mix (8 μl glutamate developer, 2 μl glutamate enzyme mix, and 90 μl assay buffer), and incubated for 30 min at 37 °C, and the OD value was measured at 450 nm by a microplate reader. A glutamate standard curve is plotted relating the OD value to the concentration of standard. The glutamate concentration of

each test sample was obtained from the standard curve and represented as micromoles per liter.

Quantitative Real-Time Polymerase Chain Reaction

The mRNA levels of inflammatory factor COX-2, CINC-1, IL-1β, IL-6, iNOS, ICAM-1, MCP-1, MIP-2, and TNF-α were quantified by quantitative real-time polymerase chain reaction (RT-qPCR) according to our previous study [20]. The right hemispheres were harvested at 24 h after SAH. Total RNA of cerebral cortex was extracted with TRIzol Reagent (Life Technologies). The concentration of RNA was measured by spectrophotometric analysis (OD260/280). Then, RNA was reverse-transcribed to cDNA with PrimeScript reverse transcriptase reagent (Takara Bio). RT-qPCR was performed with CFX96 real-time PCR detection system (Bio-Rad), applying real-time SYBR Green PCR technology. The reaction mixture (25 μl) contained cDNA (1 μl), forward and reverse primers (each 1 μl, 10 μM), SYBR Green (12.5 μl), and nuclease-free water (9.5 μl). The primer sequences of inflammatory factor were selected according to the previous study [13, 20, 22], as shown in Table 1. At 95 °C for 30 s, 38 PCR repeats were performed, each repeat consisting of a denaturation step (95 °C, 5 s) and an annealing step (60 °C, 30 s). Relative change in mRNA expression was evaluated by using the $2^{-\Delta\Delta Cq}$ method.

Enzyme-Linked Immunosorbent Assay

The right hemispheres were harvested at 24 h following SAH and performed according to our previous study [20, 23]. Cortical tissues were homogenized and centrifuged. BCA protein assay kit (Tiangen) was used to determine the protein concentration of the supernatant. The contents of IL-1β, IL-6, TNF-α, MDA, 3-NT, and 8-OHDG were quantified using enzyme-linked immunosorbent assay (ELISA) kit according to the manufacturer's instructions (IL-1β, IL-6, and TNF-α kit, MultiSciences; 3-NT and 8-OHDG kit, Cell Biolabs; MDA kit, Jiancheng Bioengineering Institute). The concentration was represented as IL-1β, IL-6, and TNF-α, in nanograms per gram; 3-nitrotyrosine, in nanomoles per gram ; 8-OHDG, in nanograms per gram; and MDA, in nanomoles per gram.

Immunohistological Staining of ED-1

Immunohistological staining was performed according to our previous study [20, 23]. Rat was anesthetized and perfused transcardially with PBS followed by 4 % paraformaldehyde at 24 h after surgery. Then, the brain was fixed in 4 % paraformaldehyde for 6 h followed by 30 % sucrose for 72 h at 4 °C. Brain section (20 μm) was incubated in blocking buffer for 30 min. Section was incubated at 4 °C in primary antibody ED-1(1:100, Millipore) for 16 h. Then, section was washed with PBS, followed by secondary antibody Alexa Fluor 568 (1:200, Life Technologies) for 2 h at room temperature, and washed again with PBS. Section was cover-slipped with anti-fading solution and viewed under a confocal microscope (Nikon), and images were taken using constant parameters.

Measurement of ROS Level, MPO, LDH, SOD, GSH-Px, and Catalase Activity and Release of Cytochrome C of Brain Cortex

Reactive oxygen species (ROS) level of the brain cortex was measured using 2′,7′-dichlorodihydrofluorescein diacetate (DCDHF-DA, Sigma) according to our previous study [23]. The myeloperoxidase (MPO), LDH, superoxide dismutase (SOD), glutathione peroxidase (GSH-Px), and catalase activity and release of cytochrome c were measured using the MPO, LDH, SOD, GSH-Px, and Catalase

Table 1 Primer sets for RT-qPCR analysis

Target gene	Forward primer (5′-3′)	Reverse primer (5′-3′)
TNF-*a*	CCCAGACCCTCACACTCAGATCAT	CAGCCTTGTCCCTTGAAGAGAA
CINC-1	CCAAAAGATGCTAAAGGGTGTCC	CAGAAGCCAGCGTTCACCA
IL-1β	CTCTGTGACTCGTGGGATGATG	CACTTGTTGGCTTATGTTCTGTCC
MCP-1	CAGAACCAGCCAACTCTCA	GTGGGGCATTAACTGCATCT
MIP-2	TTGTCTCAACCCTGAAGCCC	TGCCCGTTGAGGTACAGGAG
IL-10	CCTTACTGCAGGACTTTAAGGGTTA	TTTCTGGGCCATGGTTCTCT
COX-2	AGAAAGAAATGGCTGCAGA	GCTAGGTTTCCAGTATTGAG
iNOS	CCTTGTTCAGCTACGCCTTC	AAGGCCAAATACCGCATACC
ICAM-1	TTCACACTGAATGCCAGCCC	GTCTGCTGAGACCCCTCTTG
VCAM-1	ATTTTCTGGAGCAAGAAATT	ATGTCAGAACAACGGAATCC
IL-6	TCCTACCCCAACTTCCAATGCTC	TTGGATGGTCTTGGTCCTTAGCC
β-actin	AAGTCCCTCACCCTCCCAAAAG	AAGCAATGCTGTCACCTTCCC

Assay Kit (Jiancheng Bioengineering Institute) and Cytochrome C Releasing Apoptosis Assay Kit (BioVision), respectively. Briefly, the brain cortex of each group was homogenized and centrifuged. BCA Protein Assay Kit (Tiangen) was used to determine protein concentration of the supernatant. Then, supernatant was used for measurement according to the manufacturer's instructions. For detecting the ROS level, the brain homogenates were diluted in ice-cold HEPES-Tyrode buffer (145 mM NaCl, 2 mM $CaCl_2$, 1 mM $MgCl_2$, 5 mM KCl, 5 mM glucose, 5 mM HEPES, pH 7.6) to obtain a final concentration of 5 μg protein/μl. Then, 225 μl homogenates and 2.5 μl of DCDHF-DA (final concentration 10 μM) were added into a 96-well plate at 37 °C for 30 min in the dark place, and then fluorescence was measured (Exλ = 488 nm, Emλ = 520 nm) using a SpectraMax Microplate Reader (Molecular Devices). ROS production represented as picomoles per milligram of protein per minute. The MPO, LDH, SOD, and GSH-Px activity of each group represented as units per milligram or units per gram, the catalase activity represented as nanomoles per milligram of protein per minute, and the release of cytochrome c expresses as nanograms per gram.

Statistical Analysis

Data was presented as mean ± SEM (std. error of mean). The protein band density values of Western blot was normalized to the mean value of the sham group. Statistical analysis was performed using the GraphPad Software Prism. Statistical evaluation was processed by one-way ANOVA (and nonparametric) analysis followed by Tukey's Multiple Comparison Tests. A value of $P < 0.05$ was indicated statistically significant.

Result

Characterization of Cur-NPs

To improve bio-availability of curcumin, we used PLGA for synthesis of Cur-NPs by solvent evaporation method (Fig. 1a). Curcumin is insoluble in water, while Cur-NPs exhibited good water solubility (Fig. 1a). When observed under TEM that Cur-NPs exhibited a spherical shape (Fig. 1b). Drug release studies showed that almost 71.7 ± 4.1 % of curcumin was released in the first 12 h followed by a slow release phase releasing up to 85.1 ± 3.5 % in the next 36 h (Fig. 1c). The average particle size, entrapment efficiency, zeta-potential, and drug loading of Cur-NPs are 220 ± 25 nm, 81.7 ± 4.6 %, −20.6 ± 1.9 mV, and 16.3 ± 1.4 %, respectively (Fig. 1d).

Physiological Parameters, Grading, and Mortality of Experimental SAH

There was no significant difference in physiological parameters (mean arterial blood pressure, body temperature, body weight, and arterial blood gases) between experimental groups (data not shown). Subarachnoid blood clots were observed around the circle of Willis, brainstem, and basilar arteries following SAH (Fig. 2a).

SAH grades were similar between the vehicle, curcumin (150, 300 mg/kg), and Cur-NP (10, 20 mg/kg)-treated SAH group at 24 h (Fig. 2b), suggesting that variation in SAH size cannot confound conclusion.

Mortality rates at 24 and 48 h in each group were as follows: sham group 0 % (0/18) and 0 % (0/18), vehicle-treated SAH group 33.3 % (6/18) and 50 % (9/18), curcumin (150 mg/kg)-treated SAH group 22.2 % (4/18) and 33.3 % (6/18), curcumin (300 mg/kg)-treated SAH group 16.7 % (3/18) and 27.8 % (5/18), Cur-NP (10 mg/kg)-treated SAH group 16.7 % (3/18) and 27.8 % (5/18), and Cur-NP (20 mg/kg)-treated SAH group 11.1 % (2/18) and 22.2 % (4/18), respectively (Fig. 2c). These results suggest that curcumin or Cur-NPs reduce the mortality after SAH.

Curcumin or Cur-NPs Significantly Improved Neurological Function, Alleviated Brain Edema, and Reduced BBB Permeability After SAH

To evaluate the neuroprotective effect of curcumin or Cur-NPs on SAH, neurological scores were conducted at 24 h after SAH via the modified Garcia score system. The average neurological score in the vehicle-treated SAH group was remarkably decreased when compared to the sham-operated group (Fig. 2d). The neurological score of curcumin (150, 300 mg/kg) or Cur-NPs (10, 20 mg/kg) significantly increased compared to that of the vehicle-treated SAH group (Fig. 2d).

Global edema is an independent risk factor for high mortality and poor outcome following SAH [24]. In this study, brain edema was evaluated at 24 h after SAH via the wet weight/dry weight method. There was no significant change of brain water content in the cerebellum or brain stem after SAH. Brain water content of the left and right hemispheres in the vehicle-treated SAH group was significantly increased compared with that of the sham-operated group (Fig. 2e). Curcumin (150, 300 mg/kg) or Cur-NPs (10, 20 mg/kg) significantly decreased the brain water content compared to the vehicle-treated SAH group (Fig. 2e).

BBB permeability was evaluated by EB dye extravasation of brain at 24 h following SAH. The amount of extravasated EB dye was significantly increased in the vehicle-treated SAH group compared with that of the sham-operated group (Fig. 2f). Curcumin (150, 300 mg/kg) or Cur-NPs (10,

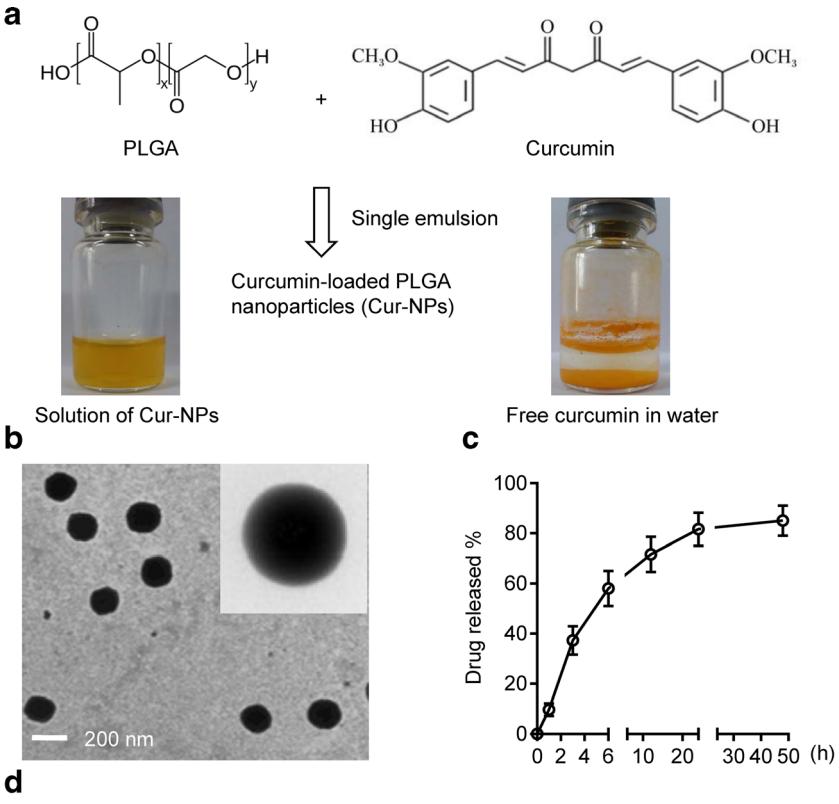

d

Particle	Average particle size	Entrapment efficiency	Zeta-potential	Drug loading
Cur-NPs	220 ± 25 nm	81.7 ± 4.6 %	-20.6 ± 1.9 mv	16.3 ± 1.4 %

Fig. 1 Physicochemical characteristics of Cur-NPs. **a** Schematic diagram of curcumin-loaded PLGA nanoparticle preparation; curcumin was encapsulated in PLGA via the single emulsion. **b** Representative TEM pictures show the morphology (spherical shape) of Cur-NPs. **c** In vitro release of curcumin from the Cur-NPs in 50 % ethanol at 37 °C; the *bars* represent the mean ± SEM from three different experiments. **d** The average particle, entrapment efficiency, zeta-potential, and drug loading of Cur-NPs. The values represent the mean ± SEM

20 mg/kg) significantly reduced the amount of extravasated EB dye compared to the vehicle-treated SAH group (Fig. 2f).

Taken together, these results indicated that impaired neurological function, brain edema, and BBB permeability following SAH were lessened by curcumin (150, 300 mg/kg) or Cur-NP (10, 20 mg/kg) treatment. Next, Cur-NPs (20 mg/kg) were used in subsequent studies to explore the possible mechanism underlying BBB dysfunction.

Cur-NPs Inhibited Blood–Brain Barrier Disruption

Previous studies demonstrate that vascular endothelial growth factor (VEGF) expression increased in cortex after SAH and suppression of VEGF level attenuates BBB disruption [25, 26]. Matrix metallopeptidase-9 (MMP9) is known to potentially mediate degradation collagen IV and lead to BBB disruption by degrading tight junction proteins (such as claudin-5, occludin, and ZO-1) after SAH [26, 27]. In this study, expression of VEGF and MMP9 increased by 161 ± 13 and 252 ± 19 % at 24 h after SAH when compared with that of the sham-operated group (Fig. 3a, b), and 121 ± 10 and 186 ± 12 % were detected in the Cur-NP (20 mg/kg)-treated SAH group (Fig. 3a, b). Protein expressions of claudin-5, occludin, and ZO-1 were significantly decreased at 24 h after SAH (Fig. 3a, b), whereas administration of Cur-NPs (20 mg/kg) increased the claudin-5, occludin, and ZO-1 expression (Fig. 3a, b). These results suggest that Cur-NP (20 mg/kg) administration attenuates BBB disruption at 24 h after SAH by preventing expression of VEGF and MMP9 and the disruption of tight junction proteins ZO-1, occludin, and claudin-5.

Cur-NPs Significantly Increased the EAAT2 Expression and Reduced Glutamate Concentration in CSF After SAH

Accumulated evidence suggests that glutamate, a major excitatory transmitter, is elevated in CSF after SAH, which has an important role in BBB disruption and neuronal death [5, 28]. EAAT2, a predominant member of the functional glutamate transporters, is essential for maintaining a low extracellular glutamate level and for preventing glutamate neurotoxicity [29]. In this study, expression of EAAT2 was significantly decreased by 48.6 ± 4.3 % at 24 h after SAH (Fig. 4a), whereas administration of Cur-NPs (20 mg/kg) increased the EAAT2 expression (Fig. 4a). Significant higher glutamate concentration of CSF was detected at 24 and 48 h after SAH when compared with that of the sham-operated group (Fig. 4b), whereas administration of Cur-NPs (20 mg/kg) attenuated this increase (Fig. 4b).

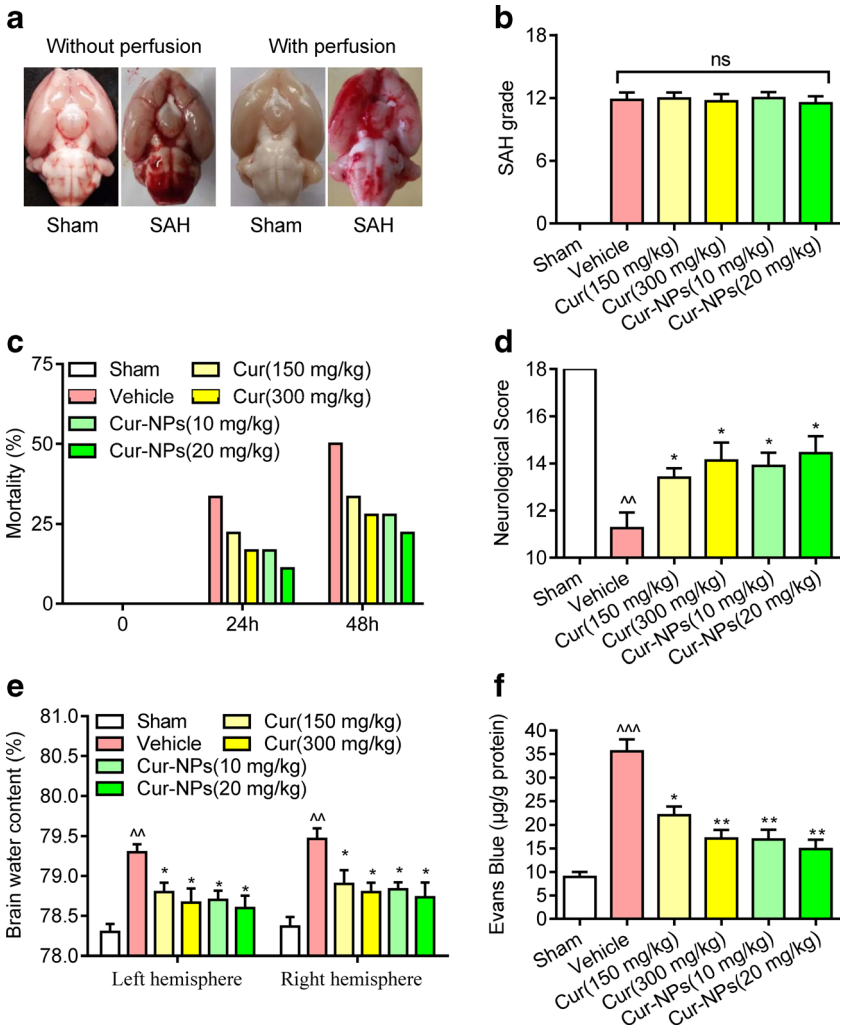

Fig. 2 Effects of curcumin and Cur-NP treatment on SAH grading, mortality modified Garcia score, brain water content, and BBB permeability at 24 h after SAH. **a** Representative images show rat brain of sham and SAH group without or with perfusion. **b** Similar SAH grading is observed in sham group ($n = 18$); vehicle ($n = 18$), curcumin (150, 300 mg/kg, $n = 18$), and Cur-NP (10, 20 mg/kg, $n = 18$)-treated SAH group. **c** Curcumin (150, 300 mg/kg) or Cur-NPs (10, 20 mg/kg) reduce mortality after SAH ($n = 18$). **d** Curcumin (150, 300 mg/kg) or Cur-NPs (10, 20 mg/kg) increase modified Garcia score at 24 h after SAH ($n = 6$). **e** Curcumin (150, 300 mg/kg) or Cur-NPs (10, 20 mg/kg) decrease brain water content in left and right hemisphere at 24 h after SAH (n = 6). **f** Curcumin (150, 300 mg/kg) or Cur-NPs (10, 20 mg/kg) decrease Evans blue extravasation at 24 h after SAH ($n = 6$). The *bars* represent the mean ± SEM. $^{\wedge\wedge}p < 0.01$ or $^{\wedge\wedge\wedge}p < 0.001$ vs sham; $^{*}p < 0.05$ or $^{**}p < 0.01$ vs vehicle

Cur-NPs Suppressed Inflammatory Response After SAH

To assess the effect of Cur-NPs on SAH-induced neuroinflammation in brain, we measured the mRNA expression of several chemokines and cytokines in the right hemisphere at 24 h after SAH. Intracellular adhesion molecule-1 (ICAM-1) and vascular cell adhesion molecule-1 (VCAM-1) were reported to play a role in leukocyte adhesion and the infiltration

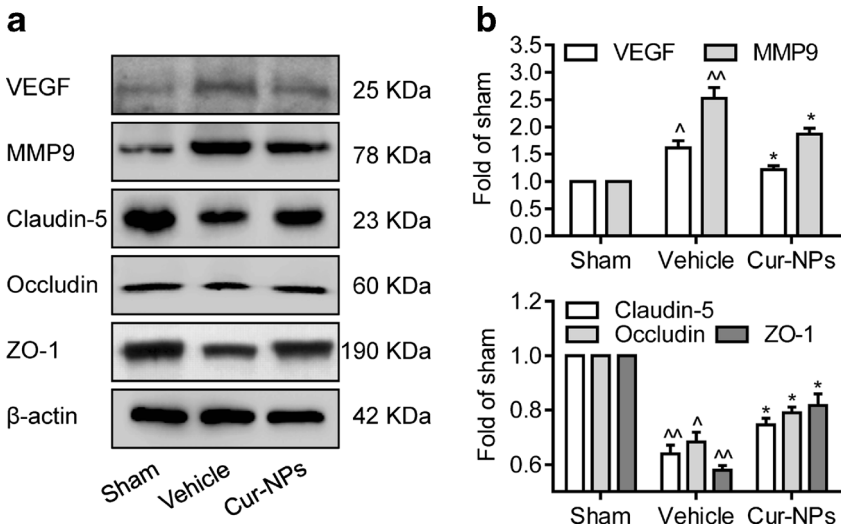

Fig. 3 **a** Representative Western blots show VEGF, MMP9, claudin-5, occludin, and ZO-1 expression of right hemisphere at 24 h after surgery in sham-operated group, vehicle, or Cur-NP (20 mg/kg)-treated SAH group ($n = 3$). **b** The relative densities of protein bands were analyzed and normalized to β-actin. The values are expressed as fold of the sham group ($n = 3$). $^{\wedge}p < 0.05$ or $^{\wedge\wedge}p < 0.01$ vs sham; $^{*}p < 0.05$ vs vehicle. The *bars* represent the mean ± SEM

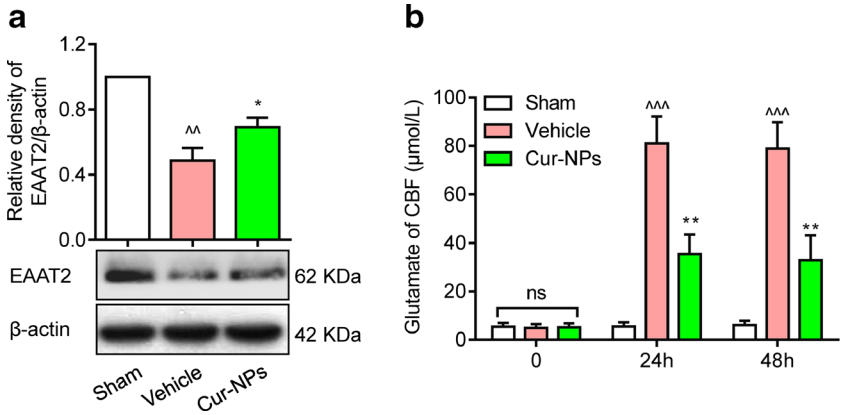

Fig. 4 **a** Representative western blots show EAAT2 expression of the right hemisphere at 24 h after surgery in the sham-operated group, vehicle, or Cur-NP (20 mg/kg)-treated SAH group ($n = 3$). The relative density EAAT2 was analyzed and normalized to β-actin. **b** Glutamate concentration of CSF at 24 and 48 h after surgery in sham-operated group, vehicle, or Cur-NP (20 mg/kg)-treated SAH group ($n = 6$). The relative content of glutamate is expressed as fold of the sham group. $^{\wedge\wedge}p < 0.01$ or $^{\wedge\wedge\wedge}p < 0.001$ vs sham; $^{*}p < 0.05$ or $^{**}p < 0.01$ vs vehicle. The *bars* represent the mean ± SEM

of macrophage/microglia and neutrophil into blood vessel adventitia after SAH [30, 31]. The mRNA expressions of ICAM-1 and VCAM-1 were significantly increased in the right hemisphere at 24 h after SAH when compared to the sham-operated group (Fig. 5a), whereas administration of Cur-NPs (20 mg/kg) could block the SAH-elevated mRNA expression of ICAM-1 and VCAM-1 (Fig. 5a). Migration and activation of macrophage/microglia, monocytes, and neutrophil in the brain contribute to neuroinflammatory response in acute stage after SAH. Key chemokines elevated after SAH include monocyte chemotactic protein-1 (MCP-1), macrophage inhibitory protein-2 (MIP-2), and chemokine-induced

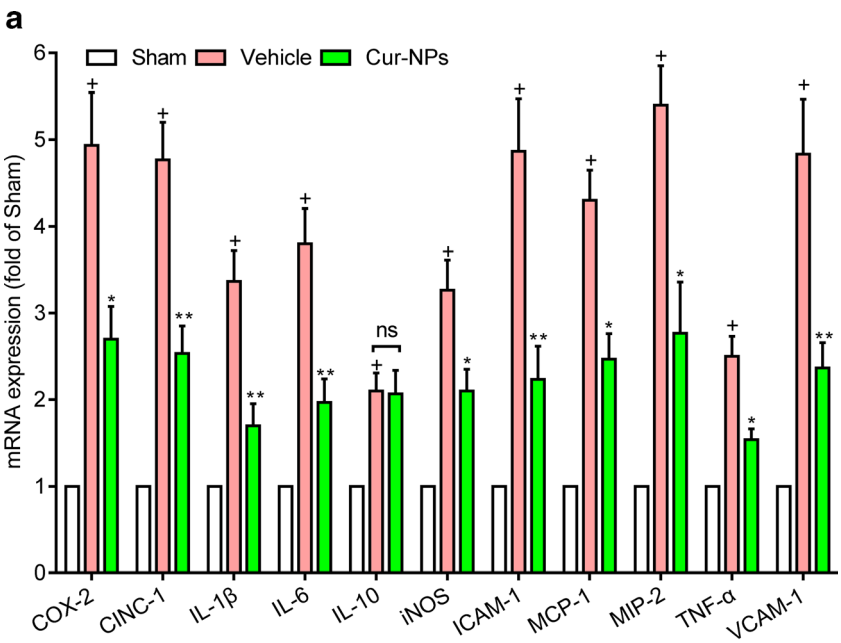

b

	n	Sham	Vehicle	Cur-NPs
IL-1β (ng/g)	6	21.68 ± 2.32	57.32 ± 5.89$^{\wedge\wedge}$	33.71 ± 4.41*
IL-6 (ng/g)	6	35.02 ± 6.79	81.33 ± 6.08$^{\wedge\wedge\wedge}$	57.06 ± 5.29**
TNF-α (ng/g)	6	5.07 ± 1.21	13.13 ± 1.18$^{\wedge\wedge\wedge}$	8.31 ± 0.82**
MPO activity (U/mg)	6	0.16 ± 0.02	0.37 ± 0.04$^{\wedge\wedge}$	0.24 ± 0.03*

Fig. 5 **a** The mRNA levels of VCAM-1, TNF-α, MIP-2, MCP-1, ICAM-1, iNOS, IL-10, IL-6, IL-1β, CINC-1, and COX-2 in the right hemisphere at 24 h after surgery in the sham-operated group, vehicle, or Cur-NP (20 mg/kg)-treated SAH group ($n = 6$). The relative mRNA is expressed as fold of sham group. $^{+}p < 0.001$ vs sham; $^{*}p < 0.05$ or $^{**}p < 0.01$ vs vehicle; *ns* no significant. The *bars* represent the mean ± SEM. **b** The protein level of IL-1β, IL-6, and TNF-α, and MPO activity in the right hemisphere at 24 h after surgery in the sham-operated group, vehicle, or Cur-NP (20 mg/kg)-treated SAH group ($n = 6$). $^{\wedge\wedge}p < 0.01$ or $^{\wedge\wedge\wedge}p < 0.001$ vs sham; $^{*}p < 0.05$ or $^{**}p < 0.01$ vs vehicle. The *bars* represent the mean ± SEM

neutrophil chemoattractant-1 (CINC-1), involving migration of macrophage/microglia and neutrophil to the injured site of the brain [22, 32]. The mRNA expressions of chemokine MCP-1, MIP-2, and CINC-1 were significantly increased in the right hemisphere at 24 h after SAH when compared with that of the sham-operated group (Fig. 5a), whereas administration of Cur-NPs (20 mg/kg) could block the SAH-elevated mRNA expression of MCP-1, MIP-2, and CINC-1 (Fig. 5a). Evidence has shown that the cyclooxygenase-2 (COX-2) and inducible nitric oxide synthase (iNOS) play a crucial role in brain inflammation [33, 34]. In this study, mRNA expressions of COX-2 and iNOS were significantly increased in the right hemisphere at 24 h after SAH as compared with that of the sham-operated group (Fig. 5a), while administration of Cur-NPs (20 mg/kg) inhibited the SAH-elevated mRNA expression of COX-2 and iNOS (Fig. 5a). Next, we measured the protein and mRNA levels of interleukin-1β (IL-1β), IL-6, and tumor necrosis factor α (TNF-α) which are known to be the most important proinflammatory cytokines in experimental SAH model and in human SAH pathology [8]. The protein and mRNA levels of IL-1β, IL-6, and TNF-α were significantly increased in the right hemisphere at 24 h after SAH when compared with that of the sham-operated group, whereas administration of Cur-NPs (20 mg/kg) could block the SAH-elevated protein and mRNA levels of IL-1β, IL-6, and TNF-α (Fig. 5a, b). Interestingly, IL-10, which is an anti-inflammatory cytokine, was significantly increased after SAH [22], but administration of Cur-NPs (20 mg/kg) cannot block the SAH-elevated mRNA expression of IL-10 (Fig. 5a). The number of granulocytes has been demonstrated to be linearly related to the MPO activity, which was selected as a quantitative readout for granulocyte influx after SAH [22]. In this study, MPO activity increased in the right hemisphere at 24 h after SAH compared with that of the sham-operated group (Fig. 5b), which indicates robust granulocyte influx following SAH. However, Administration of Cur-NPs (20 mg/kg) significantly reduced SAH-elevated MPO activity (Fig. 5b). Moreover, the number of ED-1 (a well-known marker of activated microglia/macrophage) positive cells and expression of ED-1 were increased in the right hemisphere at 24 h after SAH compared with that of the sham-operated group (Fig. 6a–c), which indicates robust microglia activation following SAH. However, administration of Cur-NPs (20 mg/kg) significantly reduced the number of ED-1 positive cells and expression of ED-1 in comparison with the vehicle-treated SAH group (Fig. 6a–c). These results indicate that Cur-NPs attenuate the neuroinflammation after SAH.

Cur-NPs Hindered Oxidative Stress After SAH

Oxidative stress reflects an imbalance between free radical productions, especially ROS, and plays an important role in EBI after SAH [7]. Mounting evidence supports that ROS are a key mediator of SAH pathogenesis, derived from the leakage of superoxide anion in disrupted mitochondria and the auto-oxidation of hemoglobin upon erythrocyte lysis [7]. Malondialdehyde (MDA), 3-nitrotyrosine (3-NT), and 8-hydroxydeoxyguanosine (8-OHDG) are known as oxidative stress markers of lipid, protein, and DNA damage, respectively. As shown in Table 2, The ROS, MDA, 3-NT, and 8-OHDG levels were significantly increased in the right hemisphere at 24 h after SAH when compared with the sham-operated group, whereas administration of Cur-NPs (20 mg/kg) effectively inhibits the SAH-elevated levels of ROS, MDA, 3-NT, and 8-OHDG. SOD, GSH-Px, and catalase activities, which are known to be the key intrinsic anti-oxidants, protect tissues from harmful effects of ROS [7]. As shown in Table 2, the SOD, GSH-Px, and catalase activities were significantly decreased in the right hemisphere at 24 h after SAH when compared with those of the sham-operated group, whereas administration of Cur-NPs (20 mg/kg) increased the SOD, GSH-Px, and catalase activities as compared with that of the vehicle-treated SAH group. These results indicate that Cur-NPs attenuate oxidative stress after SAH.

Cur-NPs Blocked SAH-Induced Apoptosis in Rats

LDH is a very stable enzyme, generally used to evaluate the presence of damage and toxicity of cell and tissue. The balance of Bcl-2 and Bax is essential for cell survival and death. Higher expression of Bax always induced mitochondrial membrane permeabilization, release of cytochrome c, and activation of caspase-9 and caspase-3, initiating apoptosis [35]. In this study, SAH significantly increased the LDH activity and release of cytochrome c in the right hemisphere at 24 h after SAH when compared to the sham-operated group, whereas administration of Cur-NPs (20 mg/kg) decreased LDH activity and release of cytochrome c in the right hemisphere at 24 h after SAH compared with that of the vehicle-treated SAH group (Fig. 7a, b). Western blot analysis shows that SAH significantly decreased Bcl-2 expression and increased Bax and active caspase-3 expression in the right hemisphere at 24 h after SAH when compared to the sham-operated group (Fig. 7c–e). However, administration of Cur-NPs (20 mg/kg) increased Bcl-2 expression and decreased Bax and active caspase-3 expression in the right hemisphere at 24 h after SAH compared with that of the vehicle-treated SAH group (Fig. 7c–e). Furthermore, administration of Cur-NPs (20 mg/kg) increased the ratio of Bcl-2/Bax when compared to the vehicle-treated SAH group (Fig. 7f).

Discussion

Mortality rates and neurological deficits were important experimental measurements for evaluating the outcome after

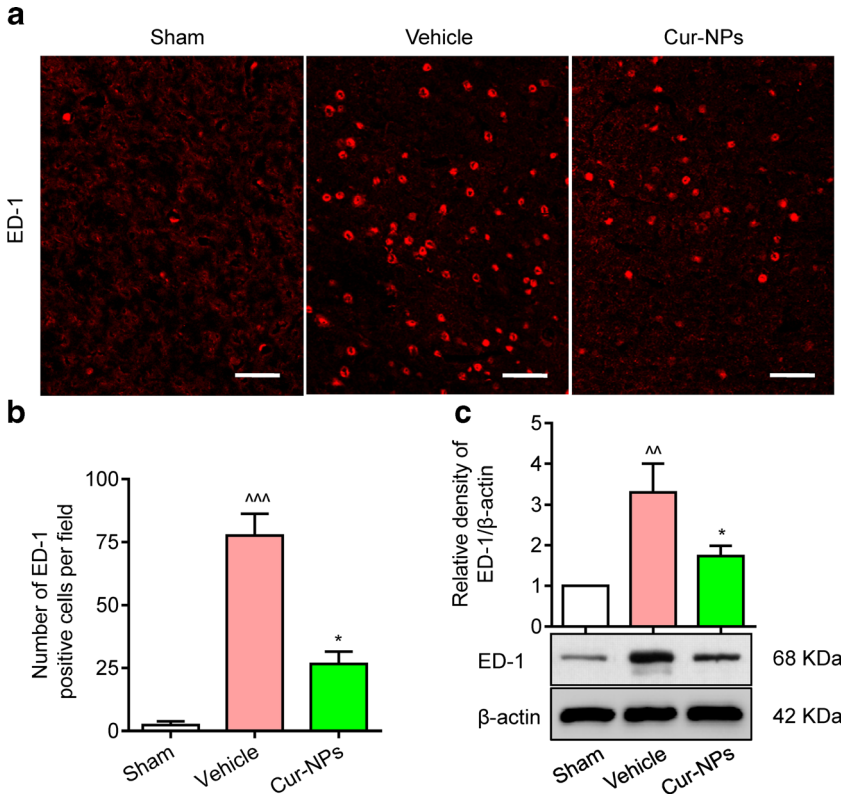

Fig. 6 **a** Typical confocal images show ED-1-immunostained right cortical sections in sham-operated group, vehicle, or Cur-NP (20 mg/kg)-treated SAH group at 24 h after surgery ($n = 3$). *Scale bar* is 100 μm. **b** Quantitative analysis of ED-1 positive cells performed by cell counting in three groups ($n = 3$). **c** Representative Western blots show expression of ED-1 in the right hemisphere at 24 h after surgery in the sham-operated group, vehicle, or Cur-NP (20 mg/kg)-treated SAH group ($n = 3$). $^{\wedge\wedge}p < 0.01$ or $^{\wedge\wedge\wedge}p < 0.001$ vs sham; $^{*}p < 0.05$ vs vehicle. The *bars* represent the mean ± SEM

SAH. Our study suggests that intraperitoneal administration of curcumin (150, 300 mg/kg) or Cur-NPs (10, 20 mg/kg) reduced the mortality and improved neurological deficits after SAH. This is similar to a previous report that intraperitoneal administration of curcumin (20 mg/kg) reduced the mortality and improved the neurological deficits in the double-hemorrhage rat SAH model [14]. It is important to clarify that different doses of curcumin provide neuroprotection following the blood injection model of mild SAH and the intracranial endovascular perforation of severe SAH. Brain edema formation is a common and important feature in EBI and is considered as a major independent risk factor for poor outcome after SAH and reflects BBB disruption [24]. Brain edema is classified into two subtypes: vasogenic and cytotoxic edema. Vasogenic brain edema refers to extracellular fluid accumulation as a result of BBB disruption, while cytotoxic brain edema defines intracellular water accumulation as the consequence of failure of ion extrusion [36]. Vasogenic and cytotoxic brain edema occur in EBI following SAH. We evaluated the brain edema of the hemisphere and observed that curcumin (150, 300 mg/kg) or Cur-NPs (10, 20 mg/kg) effectively reduced brain water content of the left and right hemispheres at 24 h after SAH. However, the applied method for measuring brain edema cannot differentiate between vasogenic and cytotoxic brain edema.

Measurement of extravasated EB dye was a reliable way to assess the extent of BBB permeability in the animal model [37]. BBB disruption occurs at about 10 min and peaks at approximately 24 h and facilitates the infiltration of serum into brain parenchyma, which leads to neuro-inflammation and edema formation [38]. Our results suggest that curcumin (150, 300 mg/kg) or Cur-NPs (10, 20 mg/kg) reduced the

Table 2 Parameters of oxidative stress after SAH or/and Cur-NP treatment

	n	Sham	Vehicle	Cur-NPs
ROS (pmol/mg protein/min)	6	7.76 ± 0.63	15.60 ± 1.65^^	10.35 ± 0.84*
MDA (nmol/g)	6	37.48 ± 3.69	76.12 ± 5.56^^	49.64 ± 4.79*
3-Nitrotyrosine (nmol/g)	6	20.20 ± 2.73	68.38 ± 5.61^^^	39.67 ± 5.15**
8-OHDG (ng/g)	6	18.62 ± 1.76	60.33 ± 5.92^^^	34.40 ± 3.85**
SOD activity (U/mg)	6	0.57 ± 0.06	0.25 ± 0.03^^	0.45 ± 0.04*
GSH-Px activity (U/mg)	6	0.96 ± 0.07	0.55 ± 0.04^^	0.83 ± 0.05*
Catalase activity (nmol/mg)	6	1.84 ± 0.09	0.93 ± 0.07^^	1.36 ± 0.08*

$^{\wedge\wedge}p < 0.01$ or $^{\wedge\wedge\wedge}p < 0.001$ vs sham; $^{*}p < 0.05$ or $^{**}p < 0.01$ vs vehicle

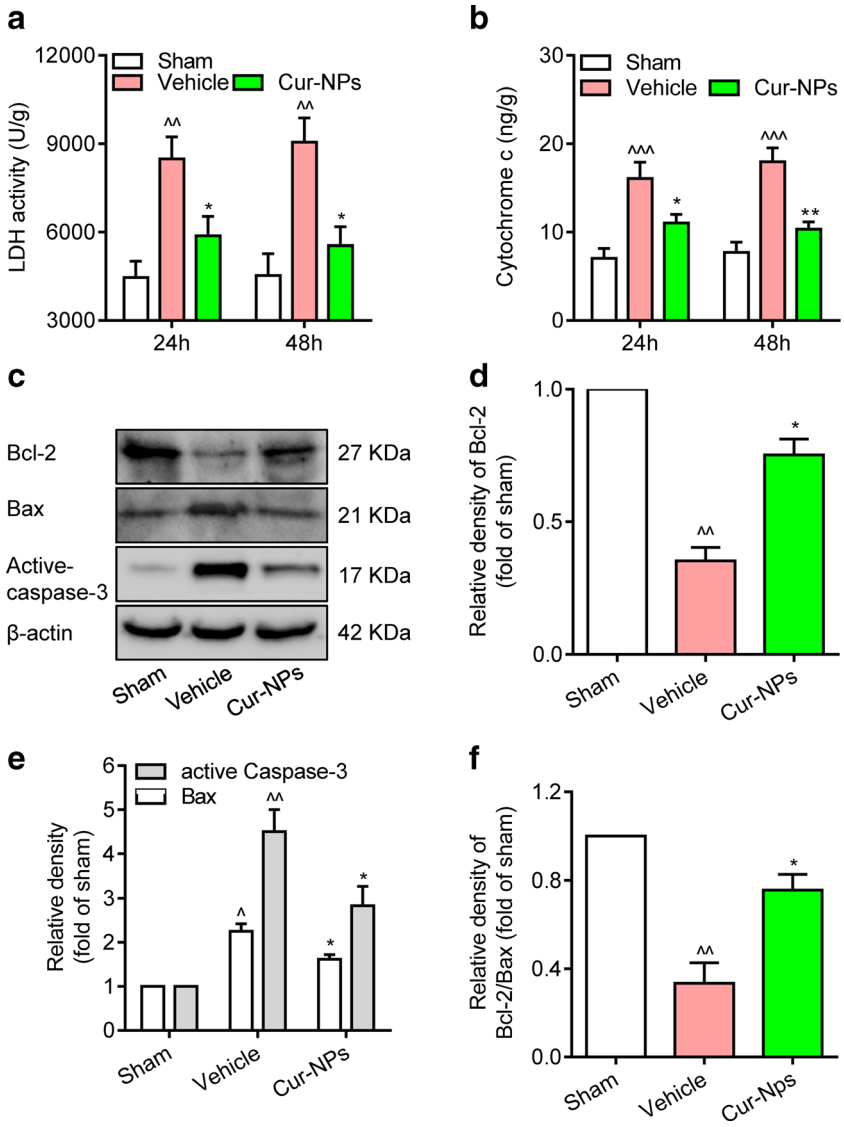

Fig. 7 **a** LDH activity, **b** cytochrome c content in right hemisphere at 24 and 48 h after surgery in the sham-operated group, vehicle, or Cur-NP (20 mg/kg)-treated SAH group ($n = 6$). **c** Representative Western blots show expression of Bcl-2, Bax, and active caspase-3 in right hemisphere at 24 h after surgery in the sham-operated group, vehicle, or Cur-NP (20 mg/kg)-treated SAH group (n = 3). **d**–**f** The relative densities of protein bands were analyzed and normalized to β-actin ($n = 3$). The values are expressed as fold of sham group. $^{\wedge}p < 0.05$, $^{\wedge\wedge}p < 0.01$ or $^{\wedge\wedge\wedge}p < 0.001$ vs sham; $^{*}p < 0.05$ or $^{**}p < 0.01$ vs vehicle. The *bars* represent the mean ± SEM

SAH-induced increase of extravasated EB dye. Altogether, these results indicate a potential neuroprotective effect of curcumin or Cur-NPs. However, the neuroprotective effect of curcumin is greatly limited by its poor brain bioavailability [10]. Accumulated evidence shows that biodegradable nanoparticle-mediated delivery of curcumin can increase the neuroprotective efficacy and decrease the required dose due to the smaller size and longer stability, and can readily diffuse across the BBB [10–12]. Indeed, our result also suggests that Cur-NPs improve the bioavailability at least tenfold when compared to native curcumin. This is similar to the previous study reports that curcumin-entrapped nanoparticles improve at least ninefold in oral bioavailability compared to curcumin [39]. Hence, we selected the Cur-NPs to explore the mechanism of BBB disruption after SAH. Previous studies demonstrate that suppression of VEGF level attenuates the BBB disruption [25, 26]. MMP9 is known to potentially mediate degradation of collagen IV and lead to BBB disruption by degrading tight junction proteins after SAH [26, 27]. Tight junction proteins claudin-5, occludin, and ZO-1 are key components of BBB integrity. Our results showed that Cur-NP treatment attenuated the BBB disruption by reducing VEGF and MMP9 expression, up-regulating the expressions of claudin-5, occludin, and ZO-1 in EBI after SAH. These results indicated that Cur-NPs may prevent BBB disruption after SAH through maintaining the tight junction proteins.

It is well established that excessive extracellular glutamate causes neurotoxicity effects via the excessive activation of ionotropic and metabotropic glutamate receptor. Mounting evidence shows that glutamate is elevated in CSF after SAH [40], which has an important role in neuronal death [5]. The inhibition of ionotropic glutamate receptor (NMDA receptor) and reduction of glutamate concentration have been shown to ameliorate the BBB disruption after SAH [28, 41]. Our result found that Cur-NPs effectively reduced the glutamate concentration of CSF at 24 and 48 h in the endovascular perforation

SAH model. This is similar to a previous report that curcumin decreased glutamate of CSF in the double-hemorrhage rat SAH model [14]. EAAT2 is essential for maintaining a low extracellular glutamate level, and increased EAAT2 expression or activity attenuates glutamate excitotoxicity [29]. Therefore, we suggest that the Cur-NPs prevent SAH-induced BBB disruption which may involve the prevention of glutamate-induced neurotoxicity.

Inflammatory responses contribute to brain edema, BBB disruption, vasospasm, and neuronal loss after SAH [8]. ICAM-1 and VCAM-1 play a role in leukocyte adhesion and the infiltration of macrophage/microglia and neutrophil into blood vessel adventitia after SAH [30, 31]; our results indicate that Cur-NPs may inhibit this adhesion and infiltration via reducing the SAH-elevated mRNA expression of ICAM-1 and VCAM-1. The chemokines MCP-1, MIP-2, and CINC-1 play a role in the migration of macrophage/microglia and neutrophil to the injured site after SAH [22, 32]; our results suggest that Cur-NPs may inhibit this migration via reducing the SAH-elevated mRNA expression of MCP-1, MIP-2, and CINC-1. The COX-2 and iNOS also play a crucial role in brain inflammation [33, 34]; our results show that Cur-NPs significantly decrease the SAH-elevated mRNA expression of COX-2 and iNOS. Measurement of MPO activity was a quantitative readout for granulocyte influx [22]; Cur-NPs significantly reduced the SAH-elevated MPO activity, suggesting inhibition of granulocyte influx after SAH. Microglia activation is correlated with the presence of later vasospasm and neurobehavioral deficits [42]. In the early phase of SAH, excessive amounts of proinflammatory cytokines released by activated microglia, together with microglial signaling-induced astrocyte cytotoxicity, become deleterious to surrounding cells [2]. We evaluated the microglia activation of the hemisphere and observed that Cur-NP treatment significantly decreases the number of activated microglia, reduces the ED-1 protein expression, and reduces the mRNA and protein level of proinflammatory cytokines IL-1β, IL-6, and TNF-α following SAH. Thus, our results indicate that Cur-NPs may prevent SAH-induced BBB disruption via reducing inflammatory responses.

Oxidative stress arises from excess free radicals and ROS, which are derived from auto-oxidation of hemoglobin and the leakage of superoxide anion in disrupted mitochondria, mediated protein breakdown, lipid peroxidation, and DNA damage, and causes the damage elements of the neurovascular unit and mediates the neuroinflammation, BBB disruption, and production of spasmogen after SAH [7]. Our result shows that Cur-NPs block the oxidative stress via reducing the SAH-elevated ROS, MDA, 3-NT, and 8-OHDG levels. Similarly, previous report shows that curcumin inhibits ROS formation and vascular hyperpermeability after haemorrhagic shock [43]. Our previous study also demonstrates that curcumin significantly suppressed oxidative damage-induced neurotoxicity in PC 12 cells [44]. Intrinsic anti-oxidant system, SOD, GSH-Px, and catalase enzyme, prevent ROS-mediated harmful effect, while a decrease in this enzyme activity is implicated in oxidative stress damage after SAH [7]. We observed that Cur-NP treatment significantly increases the SOD, GSH-Px, and catalase enzyme activity following SAH. Therefore, our results indicate that Cur-NPs may be against SAH-induced BBB disruption via blocking oxidative stress.

Cell apoptosis occurs in neuron, endothelial cell, smooth muscle, astrocyte, and oligodendrocyte following SAH; in particular, apoptosis of microvascular endothelia cell and smooth plays a significant role in BBB disruption [35]. The balance of Bcl-2 and Bax is essential for cell survival and death. Higher expression of Bax always induced mitochondrial membrane permeabilization, release of cytochrome c, and activation of caspase-9 and caspase-3, subsequently initiating apoptosis [35]. Our result found that Cur-NP treatment significantly reduced the release of cytochrome c, up-regulated Bcl-2 expression, and down-regulated the expression of Bax and active caspase-3 after SAH. These finding indicate that Cur-NPs may be against SAH-induced BBB disruption via blocking cell apoptosis. Even with the limitations of this study, our findings may provide important information about the protective effects of Cur-NPs against SAH-induced BBB disruption through preventing glutamate-induced neurotoxicity, inflammatory responses, oxidative stress, and cell apoptosis.

Conclusion

Our findings demonstrated that curcumin or Cur-NPs significantly improve neurological deficit and attenuate brain edema and BBB disruption after SAH. In addition, Cur-NPs attenuated the BBB disruption by reducing VEGF and MMP9 expression, up-regulating the expression of claudin-5, occludin, and ZO-1. Cur-NPs against SAH-induced BBB disruption may involve the prevention of glutamate-induced neurotoxicity, inflammatory responses, oxidative stress, and cell apoptosis in the endovascular perforation rat SAH model.

Acknowledgments The national natural science foundation of China (NSFC) (nos.81301018, 81501106, and 81271275) and the China Postdoctoral Science Foundation Grant (2014 M560355) supported this work.

Contributors ZZ, CF, and BS conceived the project and designed experiments. ZZ, MJ, JF, MY, ZS, YY, DL, FX, WK, HY, and LM performed the experiments; CF and BS analyzed the results. ZZ and CF wrote the manuscript. All authors read and approved the final manuscript.

Compliance with Ethical Standards

Conflict of interest The authors declare that they have no conflict of interest.

References

1. Macdonald RL (2014) Delayed neurological deterioration after subarachnoid haemorrhage. Nat Rev Neurol 10(1):44–58. doi:10.1038/nrneurol.2013.246
2. Sehba FA, Hou J, Pluta RM, Zhang JH (2012) The importance of early brain injury after subarachnoid hemorrhage. Prog Neurobiol 97(1):14–37. doi:10.1016/j.pneurobio.2012.02.003
3. Fujii M, Yan J, Rolland WB, Soejima Y, Caner B, Zhang JH (2013) Early brain injury, an evolving frontier in subarachnoid hemorrhage research. Transl Stroke Res 4(4):432–446. doi:10.1007/s12975-013-0257-2
4. Chen S, Feng H, Sherchan P, Klebe D, Zhao G, Sun X, Zhang J, Tang J et al (2014) Controversies and evolving new mechanisms in subarachnoid hemorrhage. Prog Neurobiol 115:64–91. doi:10.1016/j.pneurobio.2013.09.002
5. Wu CT, Wen LL, Wong CS, Tsai SY, Chan SM, Yeh CC, Borel CO, Cherng CH (2011) Temporal changes in glutamate, glutamate transporters, basilar arteries wall thickness, and neuronal variability in an experimental rat model of subarachnoid hemorrhage. Anesth Analg 112(3):666–673. doi:10.1213/ANE.0b013e318207c51f
6. Lai TW, Zhang S, Wang YT (2014) Excitotoxicity and stroke: identifying novel targets for neuroprotection. Prog Neurobiol 115:157–188. doi:10.1016/j.pneurobio.2013.11.006
7. Ayer RE, Zhang JH (2008) Oxidative stress in subarachnoid haemorrhage: significance in acute brain injury and vasospasm. Acta Neurochi Suppl 104:33–41
8. Miller BA, Turan N, Chau M, Pradilla G (2014) Inflammation, vasospasm, and brain injury after subarachnoid hemorrhage. BioMed Res Int 2014:384342. doi:10.1155/2014/384342
9. Noorafshan A, Ashkani-Esfahani S (2013) A review of therapeutic effects of curcumin. Curr Pharm Des 19(11):2032–2046
10. Tsai YM, Chien CF, Lin LC, Tsai TH (2011) Curcumin and its nano-formulation: the kinetics of tissue distribution and blood–brain barrier penetration. Int J Pharm 416(1):331–338. doi:10.1016/j.ijpharm.2011.06.030
11. Xie X, Tao Q, Zou Y, Zhang F, Guo M, Wang Y, Wang H, Zhou Q et al (2011) PLGA nanoparticles improve the oral bioavailability of curcumin in rats: characterizations and mechanisms. J Agric Food Chem 59(17):9280–9289. doi:10.1021/jf202135j
12. Khalil NM, do Nascimento TC, Casa DM, Dalmolin LF, de Mattos AC, Hoss I, Romano MA, Mainardes RM (2013) Pharmacokinetics of curcumin-loaded PLGA and PLGA-PEG blend nanoparticles after oral administration in rats. Colloids Surf B: Biointerfaces 101:353–360. doi:10.1016/j.colsurfb.2012.06.024
13. Wakade C, King MD, Laird MD, Alleyne CH Jr, Dhandapani KM (2009) Curcumin attenuates vascular inflammation and cerebral vasospasm after subarachnoid hemorrhage in mice. Antioxid Redox Signal 11(1):35–45. doi:10.1089/ars.2008.2056
14. Kuo CP, Lu CH, Wen LL, Cherng CH, Wong CS, Borel CO, Ju DT, Chen CM et al (2011) Neuroprotective effect of curcumin in an experimental rat model of subarachnoid hemorrhage. Anesthesiology 115(6):1229–1238. doi:10.1097/ALN.0b013e31823306f0
15. Chang CZ, Wu SC, Lin CL, Kwan AL (2015) Curcumin, encapsulated in nano-sized PLGA, down-regulates nuclear factor kappaB (p65) and subarachnoid hemorrhage induced early brain injury in a rat model. Brain Res 1608:215–224. doi:10.1016/j.brainres.2015.02.039
16. Sugawara T, Ayer R, Jadhav V, Zhang JH (2008) A new grading system evaluating bleeding scale in filament perforation subarachnoid hemorrhage rat model. J Neurosci Methods 167(2):327–334. doi:10.1016/j.jneumeth.2007.08.004
17. Peng SF, Lee CY, Hour MJ, Tsai SC, Kuo DH, Chen FA, Shieh PC, Yang JS (2014) Curcumin-loaded nanoparticles enhance apoptotic cell death of U2OS human osteosarcoma cells through the Akt-Bad signaling pathway. Int J Oncol 44(1):238–246. doi:10.3892/ijo.2013.2175
18. Doggui S, Sahni JK, Arseneault M, Dao L, Ramassamy C (2012) Neuronal uptake and neuroprotective effect of curcumin-loaded PLGA nanoparticles on the human SK-N-SH cell line. J Alzheimer's Dis: JAD 30(2):377–392. doi:10.3233/JAD-2012-112141
19. Tiwari SK, Agarwal S, Seth B, Yadav A, Nair S, Bhatnagar P, Karmakar M, Kumari M et al (2014) Curcumin-loaded nanoparticles potently induce adult neurogenesis and reverse cognitive deficits in Alzheimer's disease model via canonical Wnt/beta-catenin pathway. ACS Nano 8(1):76–103. doi:10.1021/nn405077y
20. Zhang ZY, Sun BL, Liu JK, Yang MF, Li DW, Fang J, Zhang S, Yuan QL et al (2015) Activation of mGluR5 attenuates microglial activation and neuronal apoptosis in early brain injury after experimental subarachnoid hemorrhage in rats. Neurochem Res 40(6):1121–1132. doi:10.1007/s11064-015-1572-7
21. Zhang ZY, Yang MF, Wang T, Li DW, Liu YL, Zhang JH, Sun BL (2015) Cysteamine alleviates early brain injury via reducing oxidative stress and apoptosis in a rat experimental subarachnoid hemorrhage model. Cell Mol Neurobiol 35(4):543–553. doi:10.1007/s10571-014-0150-x
22. Kooijman E, Nijboer CH, van Velthoven CT, Mol W, Dijkhuizen RM, Kesecioglu J, Heijnen CJ (2014) Long-term functional consequences and ongoing cerebral inflammation after subarachnoid hemorrhage in the rat. PLoS ONE 9(6), e90584. doi:10.1371/journal.pone.0090584
23. Zhang ZY, Sun BL, Yang MF, Li DW, Fang J, Zhang S (2015) Carnosine attenuates early brain injury through its antioxidative and anti-apoptotic effects in a rat experimental subarachnoid hemorrhage model. Cell Mol Neurobiol 35(2):147–157. doi:10.1007/s10571-014-0106-1
24. Claassen J, Carhuapoma JR, Kreiter KT, Du EY, Connolly ES, Mayer SA (2002) Global cerebral edema after subarachnoid hemorrhage: frequency, predictors, and impact on outcome. Stroke; J Cereb Circ 33(5):1225–1232
25. Wu C, Hu Q, Chen J, Yan F, Li J, Wang L, Mo H, Gu C et al (2013) Inhibiting HIF-1alpha by 2ME2 ameliorates early brain injury after experimental subarachnoid hemorrhage in rats. Biochem Biophys Res Commun 437(3):469–474. doi:10.1016/j.bbrc.2013.06.107
26. Chen J, Chen G, Li J, Qian C, Mo H, Gu C, Yan F, Yan W et al (2014) Melatonin attenuates inflammatory response-induced brain edema in early brain injury following a subarachnoid hemorrhage: a possible role for the regulation of pro-inflammatory cytokines. J Pineal Res 57(3):340–347. doi:10.1111/jpi.12173
27. Scholler K, Trinkl A, Klopotowski M, Thal SC, Plesnila N, Trabold R, Hamann GF, Schmid-Elsaesser R et al (2007) Characterization of microvascular basal lamina damage and blood–brain barrier dysfunction following subarachnoid hemorrhage in rats. Brain Res 1142:237–246. doi:10.1016/j.brainres.2007.01.034
28. Boyko M, Melamed I, Gruenbaum BF, Gruenbaum SE, Ohayon S, Leibowitz A, Brotfain E, Shapira Y et al (2012) The effect of blood glutamate scavengers oxaloacetate and pyruvate on neurological outcome in a rat model of subarachnoid hemorrhage. Neurotherapeutics: J Am Soc Exp NeuroTherapeutics 9(3):649–657. doi:10.1007/s13311-012-0129-6
29. Divito CB, Underhill SM (2014) Excitatory amino acid transporters: roles in glutamatergic neurotransmission. Neurochem Int 73:172–180. doi:10.1016/j.neuint.2013.12.008
30. Lin CL, Kwan AL, Dumont AS, Su YF, Kassell NF, Wang CJ, Wu SC, Kuo CL et al (2007) Attenuation of experimental subarachnoid hemorrhage-induced increases in circulating intercellular adhesion molecule-1 and cerebral vasospasm by the endothelin-converting

enzyme inhibitor CGS 26303. J Neurosurg 106(3):442–448. doi:10.3171/jns.2007.106.3.442
31. Oshiro EM, Hoffman PA, Dietsch GN, Watts MC, Pardoll DM, Tamargo RJ (1997) Inhibition of experimental vasospasm with anti-intercellular adhesion molecule-1 monoclonal antibody in rats. Stroke; Cereb Circ 28(10):2031–2037, **discussion 2037–2038**
32. Lu H, Shi JX, Chen HL, Hang CH, Wang HD, Yin HX (2009) Expression of monocyte chemoattractant protein-1 in the cerebral artery after experimental subarachnoid hemorrhage. Brain Res 1262:73–80. doi:10.1016/j.brainres.2009.01.017
33. Ayer R, Jadhav V, Sugawara T, Zhang JH (2011) The neuroprotective effects of cyclooxygenase-2 inhibition in a mouse model of aneurysmal subarachnoid hemorrhage. Acta Neurochir Suppl 111:145–149. doi:10.1007/978-3-7091-0693-8_24
34. Zheng B, Zheng T, Wang L, Chen X, Shi C, Zhao S (2010) Aminoguanidine inhibition of iNOS activity ameliorates cerebral vasospasm after subarachnoid hemorrhage in rabbits via restoration of dysfunctional endothelial cells. J Neurol Sci 295(1–2):97–103. doi:10.1016/j.jns.2010.04.012
35. Kooijman E, Nijboer CH, van Velthoven CT, Kavelaars A, Kesecioglu J, Heijnen CJ (2014) The rodent endovascular puncture model of subarachnoid hemorrhage: mechanisms of brain damage and therapeutic strategies. J Neuroinflammation 11:2. doi:10.1186/1742-2094-11-2
36. Nag S, Manias JL, Stewart DJ (2009) Pathology and new players in the pathogenesis of brain edema. Acta Neuropathol 118(2):197–217. doi:10.1007/s00401-009-0541-0
37. Manaenko A, Chen H, Kammer J, Zhang JH, Tang J (2011) Comparison Evans Blue injection routes: Intravenous versus intraperitoneal, for measurement of blood–brain barrier in a mice hemorrhage model. J Neurosci Methods 195(2):206–210. doi:10.1016/j.jneumeth.2010.12.013
38. Tso MK, Macdonald RL (2014) Subarachnoid hemorrhage: a review of experimental studies on the microcirculation and the neurovascular unit. Transl Stroke Res 5(2):174–189. doi:10.1007/s12975-014-0323-4
39. Shaikh J, Ankola DD, Beniwal V, Singh D, Kumar MN (2009) Nanoparticle encapsulation improves oral bioavailability of curcumin by at least 9-fold when compared to curcumin administered with piperine as absorption enhancer. Eur J Pharma Sci: Off J Eur Fed Pharm Sci 37(3–4):223–230. doi:10.1016/j.ejps.2009.02.019
40. Jung CS, Lange B, Zimmermann M, Seifert V (2013) CSF and serum biomarkers focusing on cerebral vasospasm and ischemia after subarachnoid hemorrhage. Stroke Res Treat 2013:560305. doi:10.1155/2013/560305
41. Germano A, Caffo M, Angileri FF, Arcadi F, Newcomb-Fernandez J, Caruso G, Meli F, Pineda JA et al (2007) NMDA receptor antagonist felbamate reduces behavioral deficits and blood–brain barrier permeability changes after experimental subarachnoid hemorrhage in the rat. J Neurotrauma 24(4):732–744. doi:10.1089/neu.2006.0181
42. Hanafy KA (2013) The role of microglia and the TLR4 pathway in neuronal apoptosis and vasospasm after subarachnoid hemorrhage. J Neuroinflammation 10:83. doi:10.1186/1742-2094-10-83
43. Tharakan B, Hunter FA, Smythe WR, Childs EW (2010) Curcumin inhibits reactive oxygen species formation and vascular hyperpermeability following haemorrhagic shock. Clin Exp Pharmacol Physiol 37(9):939–944. doi:10.1111/j.1440-1681.2010.05414.x
44. Fu XY, Yang MF, Cao MZ, Li DW, Yang XY, Sun JY, Zhang ZY, Mao LL et al (2014) Strategy to suppress oxidative damage-induced neurotoxicity in PC12 cells by curcumin: the role of ROS-mediated DNA damage and the MAPK and AKT pathways. Mol Neurobiol. doi:10.1007/s12035-014-9021-1